Emergence and clonal expansion in Europe of *Vibrio aestuarianus* lineages pathogenic for oysters.

Aurélie Mesnil[1,2], Maude Jacquot[1], Céline Garcia[1], Delphine Tourbiez[1], Lydie Canier[1], Audrey Bidois[2], Lionel Dégremont[1], Deborah Cheslett[3], Michelle Geary[3], Alessia Vetri[4], Ana Roque[5], Dolors Furones[5], Alison Garden[6], Petya Orozova[7], Isabelle Arzul[1], Mathieu Sicard[8], Guillaume Charrière[2], Delphine Destoumieux-Garzón[2], Marie-Agnès Travers[2*]

1 ASIM, Ifremer, Station de La Tremblade, avenue de Mus du Loup, 17390 La Tremblade, France

2 IHPE, Université de Montpellier, CNRS, IFREMER, Univ Perpignan Via Domitia, Montpellier, France

3 Marine Institute MI, Rinville, Oranmore, Co. Galway, H91 R673, Ireland

4 Istituto Zooprofilattico Sperimentale delle Venezie (IZSVe), Viale dell'Università 10, 35020 Legnaro (PD), Italy

5 IRTA La Ràpita. Aquaculture Program. 43540 – San Carles de la Ràpita, Spain.

6 Marine Laboratory, Marine Scotland Science, Aberdeen, UK.

7 National Diagnostic and Research Veterinary Medical Institute, Sofia, Bulgaria.

8 ISEM, Université de Montpellier, CNRS, IRD, Montpellier, France.

* Corresponding author: marie.agnes.travers@ifremer.fr

Competing interests: The authors declare no conflict of interest.

Abstract

Crassostrea gigas oysters, with 4.7 million tons harvested per year, represent a considerable food supply worldwide. Since 2001 *Vibrio aestuarianus* has emerged as a pathogenic bacterium causing adult oyster mortality events in France and Ireland, and its impact on oyster aquaculture has increased in Europe since its reemergence in 2012. To better understand the evolutionary mechanisms leading to the emergence and persistence over time of this pathogen, we conducted a survey with national reference laboratories (NRLs) at the European scale for mollusk diseases. We analyzed genomes of *V. aestuarianus* isolated from multiple countries, since 2001, with or without bivalve mortalities, and from multiple environmental compartments. Using a combination of comparative genomics and population genetics approaches, we show that two oyster pathogen lineages have almost clonally expanded in Europe, after a probable recent selective bottleneck. Low mutation and recombination rates, as well as purifying selective pressure, have preserved virulent selected genotypes. Furthermore, we identified a specific *cus-cop*-containing island conferring copper resistance to *V. aestuarianus* that could have favored the emergence of *V. aestuarianus* pathogenic lineages adapted to oysters.

Introduction

In an increasingly connected world, marine populations appear to be under increasing threat of emerging infectious disease (EID)(1), as illustrated by the mass mortality events currently affecting corals, sea-stars, mollusks and fish (2-4). Aquaculture is particularly threatened by EID, as it is practiced in an open and highly connected environment favoring the circulation of pathogens (5). Moreover, aquacultural practices frequently result in high population densities as well as many animal transfers, which increase the risk of regular pathogen lineage introductions and dispersal (6).

49 The emergence of new diseases is linked to changes in the interactions between pathogens,
50 hosts and the environment, which are usually caused by one or more of the following
51 situations: (a) an encounter between a pathogen and a new host, *i.e.,* cross-species
52 transmission, (b) access by a pathogen to a new area, *i.e.,* introduction, and (c) the
53 acquisition by a pathogen of a new trait that increases its capacity to colonize a host, *i.e.,* its
54 adaptation to a host (7). In bacteria, trait acquisition is often achieved by horizontal transfers
55 (through transformation, conjugation or transduction) of several genes favoring rapid
56 adaptation to new niches and hosts (8). For example, in the genus *Vibrio*, one ecological
57 population from the clade Splendidus that causes oyster spat mortalities have acquired a
58 mobilisable virulence plasmid (9). Mutations and genomic rearrangements can also influence
59 host adaptation by offering new evolutionary trajectory opportunities or by causing
60 progressive loss of gene function (10). Trait acquisition can be followed by "clonal
61 expansion", *i.e.,* evolution without recombination and the spatial and temporal expansion of
62 the lineage considered (11). The most documented example is related to *V. cholerae* clonal
63 emergence after acquisition of major virulence factors, cholera toxin (CT) and toxin
64 coregulated pilus (TCP) (12). One consequence of strict clonality is the strong effect of
65 population bottlenecks and selective sweeps (a new favorable substitution or set of
66 substitutions sweeps to fixation in a population and purges variation for the entire
67 chromosome in the clonal population) in reducing genetic diversity in the resulting population
68 (13).
69
70 Oysters (*Crassostrea gigas*) are farmed worldwide and are frequently impacted by bacterial
71 pathogens of the genus *Vibrio* (14-16). Among them, *Vibrio aestuarianus* subsp. *francensis*
72 has caused recurrent mortality of adult oysters since 2001 (17). Mortality rates of
73 approximately 25% (18) have had an important economic impact, as they affect market-size
74 oysters. Having previously been restricted to France, this disease has now spread across
75 European countries (France, Italy, Ireland, and Spain) (19, 20). Strains of another *V.*
76 *aestuarianus* subspecies (subsp. *cardii*) were isolated from diseased cockles. In addition

77 strains of *V. aestuarianus* subsp. *aestuarianus* were isolated from water, sediment,
78 zooplankton and bivalve tissues (including from oysters) outside disease outbreaks (21, 22).
79 First phenotypic and genetic studies allowed to describe *V. aestuarianus* subspecies without
80 clarifying population structure (21).
81 In previous field studies, pathogenic strains of *V. aestuarianus francensis* were found to be
82 able to colonize sentinel oysters, but they remained rare in other environmental
83 compartments sampled in the oyster surroundings (sediment and water column), suggesting
84 that oysters are its preferred habitat (23). Moreover, it has been proposed that *V.*
85 *aestuarianus francensis* can persist in oyster tissues during winter (23). These observations
86 suggest strong adaptation of *V. aestuarianus francensis* to its host and raise questions about
87 host specialization for this pathogen. However, the evolutionary processes that have led to
88 the emergence and persistence of pathogenic strains in *V. aestuarianus* remain unknown,
89 and only a limited number of genomes are available, which does not reflect overall diversity
90 across diverse isolation contexts (17, 22). This lack of genomic data hinders a complete
91 understanding of the genetic diversity and population structure of *V. aestuarianus,* and
92 prevents us from uncovering the evolutionary processed underpinning the emergence of
93 pathogenic *V. aestuarianus francensis.*
94
95 In the present study, we analyzed 54 genomes of isolates collected since 2001 across
96 Europe. We combined phylogenetic and population genetic approaches to decipher
97 evolutionary processes associated with the origin of the emergence of this oyster pathogen.
98 Our study shows that bacterial strains belonging to *V. aestuarianus francensis* exhibit
99 numerous features commonly reported in specialized pathogens. In particular, our data
100 suggest the acquisition of genes involved in copper resistance as one mechanism of *V.*
101 *aestuarianus* adaptation to oysters.
102

103 ## Results

104 ### European spread of *V. aestuarianus* oyster pathogens

105 To assess the geographic distribution of pathogenic *V. aestuarianus* in Europe, a
106 questionnaire survey was sent in 2021 to all European laboratories in charge of the
107 diagnosis and surveillance of mollusk diseases (supplementary material). Eight out of the 12
108 respondent laboratories reported the detection of *V. aestuarianus* during oyster mortality
109 events. The earliest detections were reported by France and Ireland in 2001, and most
110 recent detection by country is the suspicion of the pathogen reported by Denmark in 2021
111 (fig. 1, A). An increase in the number of countries in which the bacteria was detected was
112 observed after 2011, leading to a total of 8 European countries currently reporting *V.*
113 *aestuarianus*. However, it is important to notice that the reported date of first detection could
114 be under-estimated, as implementation of surveillance and testing for the pathogen has
115 varied between countries and was only implemented in the majority of the laboratories
116 following the development of a diagnostic tool (24).

117

118 ***V. aestuarianus* diversity is structured according to environmental origin and isolation**
119 **context.** To reconstruct the overall population structure of *V. aestuarianus* in Europe, we
120 assessed genetic diversity at the whole genome level using *V. aestuarianus* isolates that
121 were as diverse as possible. Strain selection was performed to equilibrate strain origins
122 (country, year, matrix and context): we used 54 isolates that originated from 7 countries, with
123 7 contrasting environmental origins (5 bivalve species, zooplankton and free-living bacteria
124 in the water column) and from different contexts (investigation of oyster mortalities or not).
125 The considered samples were isolated between 2001 and 2021 (plus the type strain isolated
126 in 1983 in the United States). Whole genomes were sequenced and *de novo* assembled.
127 This allowed us to obtain 15 4.5-Mb complete genomes (with 2 to 4 contigs) and 39 draft

genomes (with up to 150 contigs) (supplementary table 1). Whole genomes were aligned, and relationships between isolates were studied by building a maximum likelihood phylogeny, using strain 03_008T as an outgroup (fig. 2). Globally, genomes were close to each other in the tree and showed highly similar nucleotide compositions, as indicated by average nucleotide identities (ANIs) higher than 97.1% for all pairwise comparisons (supplementary table 2).

To confirm population structure, we focused on allele frequency differences within *V. aestuarianus* genomes. We applied the linkage model of Structure to our data and identified six ancestral populations in our samples. Strains isolated during oyster mortality events (hereafter referred to as oyster clinical isolates, OCIs) were grouped into a unique population predicted to have descended from a unique ancestor (fig S1). Almost all other strains descended from multiple ancestors, including the OCI ancestor.

The OCI group was composed of two sublineages supported by a bootstrap value of 100% and named clades A (OCI_A, n = 17) and B (OCI_B, n = 8) as previously described (22) (fig. 2). To test whether OCI/No_OCI delineation correlated with *Vibrio* virulence potential, we phenotyped most isolates by using oyster experimental infections. Virulence potential perfectly matched with phylogenic delineation: the OCI clades A and B contained all virulent isolates, which induced more than 50% mortality in oysters (fig. 2).

To determine the relationships between environmental factors and observed genetic diversity, we performed principal component analysis of genetic polymorphism using 183 109 SNPs. Principal component 1 (PC1) segregated the isolates according to isolation context and environmental origin (fig 3) but not according to isolation year or isolation country. Furthermore, analysis of molecular variance (AMOVA) performed on the sequence dataset revealed that isolation context and environmental origin explained the most significant ($p < 0.005$) amounts of genetic variation (table 1). This indicated the absence of spatial and temporal delineation of the OCI group.

154 Altogether, our data show the European expansion of *V. aestuarianus* lineages pathogenic
155 to oysters that has spread without much genetic variation since the first associated oyster
156 mortality event in 2001.

157 ## Clonal expansion of *V. aestuarianus francensis* lineages

158 Recombination is an important source of genetic diversity in bacterial populations that may
159 drive the emergence of pathogens. We therefore quantified and localized recombination
160 events along *V. aestuarianus* genome alignments.
161 **The impact of recombination on OCI diversity was weak.** Recombination events were
162 almost exclusively detected outside OCIs, with, on average, 342.5 recombination events per
163 genome. In the NO_OCI alignment, 164 704 polymorphic sites are engendered by
164 recombination. In contrast, in OCI genomes, only 7.8 and 3.3 recombination events were
165 detected on average for clades A and B, respectively, generating only 5 207 and 1 232
166 polymorphic sites (0.1% of the genome nucleotides). Recombination in genomes is known to
167 generate phylogenetic inconsistencies between taxa that can be visible in a phylogenetic
168 network as the presence of alternative pathways (25). The network that we constructed from
169 the whole-genome alignment (fig S2) confirmed that recombination does not affect OCI
170 relationships, with few alternative pathways between these taxa. One known consequence of
171 the absence of recombination impacts is strong linkage between loci in non-recombinant
172 genomes (26). In OCI_A and, to a lesser extent, in OCI_B genomes, strong linkage between
173 single nucleotide polymorphisms (SNPs) was observed (fig S3). In contrast, the
174 recombination impact detected in all other genomes was confirmed with phylogenetic
175 networks, which showed inconsistencies between NO_OCI taxa (fig S2) and low linkage
176 between loci in these genomes (fig S3). However, recombination might have played a role in
177 the emergence of this pathogenic group, as 488 recombination events were detected at the
178 node corresponding to the hypothetical common ancestor of all OCI isolates (fig. 4).
179 Mutations also generated little genetic diversity among OCIs. Indeed, apart from the

180 recombinant segments, 666 and 83 polymorphic sites were observed in OCI_A and OCI_B,
181 respectively, compared with 19 775 in NO_OCI isolates.
182 Altogether, our data support the clonal expansion of two *V. aestuarianus francensis* lineages
183 that are pathogenic to oysters.
184

185 **Bottlenecks and purifying selection may limit pathogenic *V. aestuarianus***
186 **genetic diversity**

187 Selection is a major evolutionary force that controls the genetic diversity generated by
188 mutation and recombination. Here we used Tajima's D to compare the genetic diversity
189 observed in *V. aestuarianus* to the genetic diversity expected under neutral evolution and
190 constant population size.
191 The deviation from neutrality was by far the largest among the OCI_A and OCI_B and could
192 be due to a combination of recent population expansion after selective bottlenecks and
193 purifying selection, as shown by the very negative values in these two clades (fig. 5, A). To
194 determine whether the low genetic diversity of OCIs was due to demographic effects
195 (affecting whole genomes) or to selection effects (affecting some of the genes), we adopted
196 a gene-based approach to investigate selection pressures at the gene level. While most of
197 the 1 974 core genes were under neutral evolution outside of the OCI clades, the vast
198 majority were monomorphic within OCI_A and OCI_B (fig. 5 B, supplementary table 3),
199 which is consistent with the low genetic diversity observed along the alignment of complete
200 genomes (fig. 5 A). Purifying selection could also act, amplifying low genetic diversity in OCI
201 clades. Indeed, contrasting selection patterns were observed among genes in OCIs, with a
202 small portion of genes showing polymorphisms, some of which were under neutral evolution
203 and others of which were under purifying selection (fig. 5 B, supplementary table 4).
204 Overall, our data indicate that pathogenic clades of *V. aestuarianus* have expanded following
205 a selective bottleneck, as revealed by a high number of monomorphic genes. However,

206 purifying selection pressure also tends to maintain the genotype of the ancestor of these
207 groups, as indicated by variation in gene diversity patterns.
208

209 ## Oyster-pathogenic *V. aestuarianus* have a conserved pangenome

210 Considering (i) the low genetic diversity of OCIs, (ii) their restricted (currently known)
211 habitats, and (iii) the scarcity of recombination events after the expansion of the two OCI
212 clades, we hypothesized that oyster-pathogen *V. aestuarianus* exhibit a closed pangenome
213 preserved from horizontal gene transfer (HGT).
214 OCIs were found to have a closed pangenome, mainly with genes being shared between
215 them and almost no genes specific to one strain, as determined by dataset pangenome
216 analysis (fig S4). In contrast, NO_OCI strains exhibited many strain-specific genes.
217 The absence of detection of homologous recombination and the closed pangenome indicate
218 that horizontal gene exchange in the OCI clades is currently absent or transparent (if
219 identical sequences are exchanged), supporting sexual isolation. In contrast, the numerous
220 homologous recombination events detected in NO_OCI genomes, as well as the large
221 quantity of specific genes that these genomes contain, showed that NO_OCI strains do not
222 come from strictly clonal reproduction but that HGT are still frequent.
223 According to these data, the two OCI clades can be considered pathogenic clonal complexes
224 that undergo clonal reproduction with limited mutation, recombination and HGT. Such sexual
225 isolation is a hallmark of specialist pathogens, which live in a very limited number of habitats
226 and have few opportunities to exchange genetic material with other populations. This
227 strongly suggests that oyster-pathogenic *V. aestuarianus* have evolved as oyster specialists.
228

229 ## Oyster-pathogenic *V. aestuarianus* have genomic features of specialist
230 pathogens

231 We further tested the hypothesis of OCI specialization by analyzing the genomic features of
232 specialists: insertion sequences (ISs) and pseudogene enrichment (27). We found higher
233 numbers of ISs in the OCI_A and OCI_B genomes than in NO_OCI group 1 genomes
234 corresponding to strains isolated in contexts without bivalve mortality (Kruskal test, p = 0.01
235 and 0.02, respectively). Interestingly, in NO_OCI group 2 containing strains isolated during
236 cockle mortality events, ISs were more abundant than in the OCI_A and OCI_B genomes (p
237 = 0.02 and 0.03, respectively) (fig. 6). IS families were conserved between OCI genomes,
238 with most ISs belonging to the IS66, IS902 and ISAS1 families (supplementary table 5 and
239 fig S5). IS conservation in OCI clades suggests that IS enrichment and expansion in OCI
240 genomes stopped after pathogen emergence. The dynamics of the ISs appeared to be
241 different in the cockle isolates. Indeed, the number and families of ISs represented appeared
242 to be poorly conserved. We suspect that IS flux is active in cockle isolates, with both
243 horizontal exchanges and intragenomic expansion.
244 To check whether IS enrichment is involved in pseudogenization, we crossed IS and
245 pseudogene genomic coordinates and determined the number of ISs with pseudogenes
246 around them (from 2 000 bp before the IS start to 2 000 bp after the IS end) (supplementary
247 tables 6 and 7). Regardless of the genome and chromosome considered, the vast majority of
248 ISs had pseudogenes nearby.
249 IS and pseudogene enrichment supports our hypothesis of specialization of the OCI clades.

250 ## Copper resistance acquisition: One potential step in the emergence of oyster-
251 pathogenic clades

252 Trait acquisition is often the first step preceding selective bottlenecks and clonal expansion
253 of host-adapted pathogens. To identify traits that may have allowed oyster pathogen
254 emergence, we studied the *V. aestuarianus* pangenome and detected 139 genes that were

255 shared exclusively by OCI_A and OCI_B genomes. Most of them (106) were annotated as
256 hypothetical proteins. The remaining 33 genes encode proteins with functions related to
257 copper export, cell-bacteria interaction (LPS/antigen O, cell wall or peptidoglycan),
258 chemotaxis and DNA repair. The sequences of these 139 genes were identical or well
259 conserved between strains (supplementary table 8).
260 Some OCI-specific genes were located in a putative mobile genetic element (MGE), as
261 determined by crossing their coordinates with IS coordinates in an OCI genome (02_041)
262 (fig. 7 A). This putative MGE contains the genes of the Cus operon (*cusABCF,S/R)*
263 surrounded by ISs from the IS66 family (length = 15 kb), as well as the copper export genes
264 *copA* and *copG* and the regulator *cueR*, located near tn7 transposon genes (tnA, B, C and
265 E) (length = 10 kb), and is later referred to as a *cus-cop*-containing island.
266
267 The OCI ancestor could have acquired copper export genes by horizontal transfer, and
268 integration into its genome could be facilitated by its presence in the MGE. To investigate the
269 origin of *cus-cop*-containing islands, we used blast analyses of each operon and of the entire
270 region in 127 reference genomes of different *Vibrio* species (supplementary table 9 and fig
271 S6). The *cus-cop*-containing island presence is scattered along the Vibrio phylogeny and is
272 not specific of a monophyletic group. It appeared highly similar to some *V. fluvialis* and *V.*
273 *furnissii* genomic sequences with a nucleotide identity >95%. Moreover, this region was
274 close to plasmidic elements identified in *V. crassostreae* and *Vibrio* sp. dgh with a nucleotide
275 identity >89% (fig. 7B).
276 To test whether the genomic differences between the OCI and NO_OCI groups could lead to
277 phenotypic differences, we determined the copper resistance capacities of 27 *V.*
278 *aestuarianus* strains using an agar diffusion assay. Supporting our hypothesis, all OCIs (8
279 strains from OCI_ A and 5 from OCI_ B) appeared more resistant than NO_OCI strains to
280 copper in radial diffusion assays (fig. 7C).

281 ## Discussion

282 Here, we describe a genomic analysis of a *V. aestuarianus* collection isolated from multiple
283 countries, in different epidemic contexts and from multiple environments since 2001. We
284 report the European expansion and clonal evolution of two oyster-pathogenic lineages,
285 belonging to the previously described *V. aestuarianus francensis* subspecies (17).

286 *V. aestuarianus francensis* pathogenic lineages OCI_A and OCI_B appear to have emerged
287 as a consequence of the acquisition a specialized lifestyle trait. Indeed, we observed a
288 markedly low level of genetic diversity among the 25 genomes of the OCI which was
289 attributed to a low level of recombination. OCI were also characterized by a closed
290 pangenome. This led us to formulate the hypothesis of a sexual isolation of OCI, a hallmark
291 of specialized pathogens, which do not exchange genes with other bacterial populations.
292 During specialization, pathogens make the transition from facultative parasitic life to a
293 permanent association with a host. As they live continuously in a host, they can acquire
294 compounds of intermediate metabolism from this host thus often discarding genes
295 associated to biosynthetic pathways that have become facultative or redundant (25). Studies
296 on pathogen specialization have mainly focused on highly specialized intracellular bacteria,
297 often obligate parasite, which can undergo an extreme genome rationalization process (26).
298 This process implies pseudogenization of genes that have become inessentials
299 accumulating mutations or ISs, and can ultimately result in genome size reduction through
300 gene loss (27-29). As a hallmark of host specialization, pseudogenization was observed in
301 both OCI lineages. However, genome size reduction was not observed, probably because *V.*
302 *aestuarianus francensis* pathogenic lineages are not obligate parasites. Indeed, whereas
303 OCI have a restricted habitat (they are almost exclusively found in oysters), they have
304 retained the ability to replicate in the absence of their host, at least in rich medium.
305 Moreover, *V. aestuarianus francensis* have the capacity to colonize a diversity of tissues
306 inside their host, including hemolymph, gills and digestive connective tissues (23). Hence *V.*

307 *aestuarianus francensis* is adapted to diverse tissular micro-environments in line with a lower
308 degree of specialization than highly specialized obligate intracellular bacteria. While being
309 strongly associated with oysters, OCI are probably not intracellular pathogens. Indeed,
310 Labreuche *et al.* showed that an OCI strain was able to inhibit phagocytosis by oyster
311 hemocytes (30). More in depth studies on OCI microhabitats within the oyster could help to
312 elucidate their complete intra-host life cycle, and the functional roles of the gene repertoire.
313 Whether OCI_A and OCI_B occupy similar niches in infected oysters and whether they have
314 the potential to cooperate is also unknown. Neither epidemiological parameter estimation
315 (31) nor in-depth analysis of their genomes has permitted the identification of functional traits
316 specific to each lineages yet.

317

318 We showed here that the two oyster pathogen lineages have almost clonally expanded in
319 Europe, after a probable recent selective bottleneck. A key event accompanying bottleneck
320 was the acquisition of copper resistance traits, which may have contributed to the
321 emergence of the two oyster-pathogenic lineages. Similar to what is observed in OCI
322 lineages, some pathogenic monomorphic lineages are thought to have endured population
323 bottlenecks associated with the acquisition of new functions (32). Such new functions could
324 allow a bacterial lineage to colonize a new host (32). Here we highlighted that OCI strains
325 have acquired a particular genomic island containing genes involved in copper detoxification.
326 Acquisition of this genomic island is likely to have allowed a better adaptation to life in
327 oysters. Indeed, copper is a heavy metal found at high levels in coastal waters because of
328 agricultural and industrial activities (33-35), and copper can accumulate at very high
329 concentrations in oyster tissues (up to 18,000 µg/g in China (36)). In oyster tissues, copper
330 can accumulate at sites of infection in oysters (37), where it plays a major role in the
331 antimicrobial defense of the infected host as copper can kill invading microorganisms (37-
332 39). Bacteria have developed copper detoxification mechanisms which utilize the *cop* and
333 *cus* genes (40). *Cop* genes encode for primary mediators allowing initial Cu^+ translocation

334 from the cytoplasm to the periplasm. *Cus* genes encode and regulate for a CusABC system
335 that transports periplasmic copper across the cell membrane toward the extracellular
336 medium (41). Importantly, *copA* is essential for copper resistance, oyster colonization and
337 virulence in the *V. tasmaniensis* LGP32, an oyster-pathogenic strain associated to the
338 Pacific Oyster Mortality Syndrome (42). Similarly, in another oyster pathogen, *V.*
339 *crassostreae,* the deletion of the *copA* also results in virulence attenuation (14). Together
340 with those previous observations, our data support copper resistance as a common trait
341 shared by different oyster bacterial pathogens whose acquisition may be required for
342 adaptation to the oyster as a niche.

343 Here we report the clonal expansion of *V. aestuarianus francensis* OCI_A and OCI_B across
344 Europe. One scenario which has been put forward to explain the increase of *V. aestuarianus*
345 associated mortalities over the last years implies the role of another major pathogen
346 affecting *C. gigas*, the Ostreid herpes virus OsHV-1. This virus has been regularly detected
347 during spat mortality events (43), and has been associated with higher mortality rate in all
348 growing areas of *C. gigas* along the French coasts (44), since the emergence of a new
349 variant in 2008. Recently, dual infections by OsHV-1 and *V. aestuarianus* were reported in
350 French oyster farms in 2014 and 2015 (45, 46) and have also been observed in Ireland since
351 2008 (Cheslett, pers comm). Even if experimental infections combining both pathogens at
352 high doses in spat and juvenile *C. gigas* did not demonstrate a direct collaboration between
353 them (47, 48), it can be hypothesized at a population level that the virus weakens animal
354 defenses thereby contributing to amplify *V. aestuarianus* local concentrations and initiate
355 epizootic events. Overall, the higher occurrence of *V. aestuarianus* since 2012 in Europe
356 could represent collateral damage resulting from the strong impact of the virus on French
357 and European oyster populations reported since 2008.

358 When the OCI pathogenic lineages emerged and how they have spread across Europe
359 remains to be elucidated. Based on genome sequencing data, phylodynamics makes it
360 possible to date outbreaks and investigate hypotheses of pathogen introduction and spread

361 (49). However, genomic data are still missing in order to date with confidence the emergence
362 of the 2 oyster-pathogenic lineages. Still, the clonality of the lineages that have emerged
363 concomitantly in Ireland and France suggests a possible transmission route from France to
364 Ireland, which is consistent with the fact that the Irish oyster industry relies massively on
365 French spat production. Global dissemination of pathogens is a recurring problem in
366 agriculture as in aquaculture and is often favored by anthropogenic introductions through
367 infected hosts (50). Preventing pathogen spread during transfers is particularly complicated
368 in the case of *V. aestuarianus* since animals can be asymptomatic (23). This is of particular
369 concern for the oyster industry which traditionally involves multiple transfers during the
370 lifetime of an oyster. Transfers of infected animals likely explain most of the spread of
371 pathogenic *V. aestuarianus* lineages across Europe. The lack of traceability in oyster farming
372 (52) is a major factor limiting the identification of epizootic sources, routes of dispersal and
373 application of control measures in many European countries (53). Therefore, beyond
374 regulating tranfers, there is an important need to develop very sensitive detection assays to
375 monitor animal sanitary status. We believe that some OCI specific genes revealed in this
376 study, like the *cusS/R* genomic island specific to pathogenic *V. aestuarianus* could be good
377 candidates to develop new early diagnostic tools.

378

379 **Material & methods**

380 **Isolate selection**

381 The *V. aestuarianus* isolates were collected during oyster mortality events in Europe
382 between 2001 and 2020 and independently of oyster mortality events between 1983 (type
383 strain isolated in the USA) and 2021. Among the isolates obtained independently of oyster
384 mortality episodes, a portion were isolated during cockle mortality episodes, which occurred
385 in France in 2012, 2015, 2018 and 2019.

386 Isolates were collected with the help of European NRLs responsible for the diagnosis and
387 surveillance of mollusk diseases: Ifremer (France), MI (Ireland), IZSVE (Italy), IRTA (Spain),
388 Marine Scotland Science (Scotland), and NRLFMC (Bulgaria). The 54 isolates used in the
389 study are summarized in the Supplementary table 10.

390 **Illumina and PacBio whole-genome sequencing**

391 DNA was isolated from 35 strains using the NucleoSpin Tissue Kit (Macherey-Nagel)
392 following the manufacturer's guidelines, and the concentration of each sample was adjusted
393 to 0.2 ng/µl for library preparation using the Illumina Nextera XT DNA Library Preparation Kit
394 according to the manufacturer's guidelines. For each library, paired-end reads of 150 bp
395 were produced on the Illumina NextSeq 550 platform (Bio Environnement, Perpignan,
396 France). The quality of the resultant fastq files was assessed using FastQC (54). Primers,
397 Illumina adapter sequences, low-quality bases at the 3′ end of reads with Phred-scaled
398 quality scores less than 30 and reads with a length <50 bp were removed using Trim Galore
399 (55). Quality-controlled reads were *de novo* assembled using the SPAdes genome
400 assembler v3.13.1 (56) with the default kmer size and a coverage cutoff value of 20 reads
401 (57).
402 DNA was isolated from other strains using a MagAttract HMW DNA Kit (Qiagen) following
403 the manufacturer's instructions. Library preparation and sequencing on a PacBio Sequel II
404 instrument were performed with the GENTYANE INRAe platform (Clermont-Ferrand,
405 France). *De novo* genome assemblies were obtained using FLYE v2.8.3 (58). One round of
406 polishing was performed using RACON v 1.4.3 (59).
407 The assembly was evaluated with QUAST, and genome completeness was checked using
408 the BUSCO v5.1.1 (60) and vibrionales_odb10 databases as lineage datasets, including 57
409 Vibrionales as detailed in Supplementary table 11.
410 Assembly features and GenBank accession numbers are summarized in Supplementary
411 table 1.

412 ## Genome annotations

413 For each assembly, coding sequences (CDSs) were predicted using PROKKA v1.12 (61)
414 with default databases and –compliant and –rfam flags and annotation of rRNAs, tRNAs and
415 other ncRNAs enabled. Functional annotation of the detected CDSs was performed using
416 EggNog-Mapper v2.1.0 (62, 63). ISs were detected in the genomes using ISEScan v1.7 (64).
417 Pseudogene detection was performed with the GenBank files released from PROKKA with
418 PSEUDOFINDER v1.0 (65) , using the diamond flag and NCBI nonredundant database.
419 These later analyses were performed only on resolved genomes to avoid obtaining false
420 negatives in IS detection and false positives in pseudogene detection at the intercontig
421 locations.

422 ## Phylogeny and recombination analysis

423 Pairwise ANIs (%) were calculated using FastANI (66). Whole-genome alignments of the 54
424 isolate contigs were made using Progressive Mauve v13/02/2015 (67). Whole-genome
425 alignment was used to infer the maximum likelihood phylogeny using RAxML v8.2.12 with
426 the GTRGAMMA model of nucleotide substitution and 100 bootstrap replicates, with strain
427 03_008T as the outgroup. Polymorphic sites along the alignment were detected using SNP
428 sites (68).
429 To assess the influence of various structuring factors on the observed genetic diversity, we
430 performed AMOVA and principal component analysis on the sequence dataset, with
431 environmental origin, isolation context, sampling year, and country as structuring factors,
432 using the R packages *pegas, factomineR* and *factoExtra*.
433 Recombination was evaluated across this genome alignment using ClonalFrameML v1.12
434 (69). We used an extension of the standard ClonalFrame model that allows different
435 recombination parameters to be inferred on different branches of the clonal genealogy.
436 03_008T was used as a reference.

437 ### Selection analysis

438 Data were subjected to a neutrality test using Tajima's D (70) with the command tajima.test
439 in the R package *pegas* v1.1 (71). Tajima's D statistic measures the difference between two
440 statistics describing the diversity within the alignment (using π based on the average number
441 of pairwise differences among sequences and θ based on the number of segregating sites),
442 standardized by the variance of this difference. Under the neutral evolutionary model, which
443 assumes that polymorphisms segregate at mutation–drift equilibrium, Tajima's D is expected
444 to be zero. Positive Tajima's D values indicate that there is an excess of polymorphisms at
445 intermediate frequencies and is typically associated with diversifying selection. Conversely,
446 negative Tajima's D values can be the result of purifying selection or a selective sweep
447 (where a beneficial allele has recently reached fixation due to strong positive selection), both
448 of which result in an excess of weakly divergent alleles. However, both positive and negative
449 Tajima's D values can also result from demographic and epidemiological processes.

450 ### Bacterial virulence estimation by injection

451 Bacteria were grown with constant agitation at 22°C for 24 h in Zobell medium. Cultures
452 were washed by centrifugation (10 min, 1500 g) and resuspended in artificial, sterile
453 seawater to obtain OD_{600nm} = 0.1. Fifty microliters of bacterial suspensions (10^7 cfu, checked
454 by plating on Zobell agar) were injected intramuscularly into anesthetized specific pathogen-
455 free (SPF) oysters produced and maintained in the IFREMER facility (72). After injection, the
456 oysters were transferred to aquaria (10 oysters per 2.5 L aquarium, duplicate aquaria per
457 bacterial strain) containing 2 L of aerated, UV-treated seawater at 22°C and kept under static
458 conditions for 5 days.

459 ### Copper resistance phenotyping

460 Paper discs (6 mm) were loaded with $CuSO_4$ by soaking them overnight into a 50 mM $CuSO_4$
461 solution. Cells from stationary phase cultures at DO = 1 were washed twice with SSW before

being spread onto agar plates containing 15 g.L^{-1} bactopeptone and 0.5 M NaCl. Using sterile tweezers, copper-impregnated disks were placed on the bacterial lawn before incubation at 20°C. After 5 days of incubation, the diameter of the inhibition zone around the disk was measured.

Bibliographic references

1. Le Roux F, Wegner KM, Baker-Austin C, Vezzulli L, Osorio CR, Amaro C, et al. The emergence of Vibrio pathogens in Europe: ecology, evolution, and pathogenesis (Paris, 11–12th March 2015). Frontiers in microbiology. 2015;6:830.
2. Frans I, Michiels CW, Bossier P, Willems KA, Lievens B, Rediers H. *Vibrio anguillarum* as a fish pathogen: virulence factors, diagnosis and prevention. Journal of Fish Diseases. 2011;34(9):643-61.
3. Hewson I, Button JB, Gudenkauf BM, Miner B, Newton AL, Gaydos JK, et al. Densovirus associated with sea-star wasting disease and mass mortality. Proc Natl Acad Sci U S A. 2014;111(48):17278-83.
4. Lafferty KD, Kuris AM. Mass mortality of abalone Haliotis cracherodii on the California Channel Islands: tests of epidemiological hypotheses. Marine Ecology-Progress Series. 1993;96:239-.
5. Lafferty KD, Harvell CD, Conrad JM, Friedman CS, Kent ML, Kuris AM, et al. Infectious Diseases Affect Marine Fisheries and Aquaculture Economics. Annual Review of Marine Science. 2015;7(1):471-96.
6. Murray AG, Peeler EJ. A framework for understanding the potential for emerging diseases in aquaculture. Preventive Veterinary Medicine. 2005;67(2):223-35.
7. Engering A, Hogerwerf L, Slingenbergh J. Pathogen-host-environment interplay and disease emergence. Emerg Microbes Infect. 2013;2(2):e5-e.
8. Martínez JL. Bacterial pathogens: from natural ecosystems to human hosts. Environmental Microbiology. 2013;15(2):325-33.
9. Bruto M, Labreuche Y, James A, Piel D, Chenivesse S, Petton B, et al. Ancestral gene acquisition as the key to virulence potential in environmental Vibrio populations. The ISME Journal. 2018;12(12):2954-66.
10. Sheppard SK, Guttman DS, Fitzgerald JR. Population genomics of bacterial host adaptation. Nature Reviews Genetics. 2018;19(9):549-65.
11. Tibayrenc M, Ayala FJ. Reproductive clonality of pathogens: A perspective on pathogenic viruses, bacteria, fungi, and parasitic protozoa. Proceedings of the National Academy of Sciences. 2012;109(48):E3305-E13.
12. Kumar A, Das B, Kumar N. Vibrio Pathogenicity Island-1: The Master Determinant of Cholera Pathogenesis. Frontiers in cellular and infection microbiology. 2020;10:561296.
13. Smith NH, Gordon SV, de la Rua-Domenech R, Clifton-Hadley RS, Hewinson RG. Bottlenecks and broomsticks: the molecular evolution of *Mycobacterium bovis*. Nature Reviews Microbiology. 2006;4(9):670-81.
14. Bruto M, James A, Petton B, Labreuche Y, Chenivesse S, Alunno-Bruscia M, et al. *Vibrio crassostreae,* a benign oyster colonizer turned into a pathogen after plasmid acquisition. The ISME Journal. 2017;11(4):1043-52.
15. Lemire A, Goudenège D, Versigny T, Petton B, Calteau A, Labreuche Y, et al. Populations, not clones, are the unit of vibrio pathogenesis in naturally infected oysters. The ISME Journal. 2015;9(7):1523-31.
16. Petton B, Bruto M, James A, Labreuche Y, Alunno-Bruscia M, Le Roux F. *Crassostrea gigas* mortality in France: the usual suspect, a herpes virus, may not be the killer in this polymicrobial opportunistic disease. Frontiers in microbiology. 2015;6:686.

17. Garnier M, Labreuche Y, Nicolas JL. Molecular and phenotypic characterization of *Vibrio aestuarianus* subsp. *francensis* subsp. nov., a pathogen of the oyster *Crassostrea gigas*. Syst Appl Microbiol. 2008;31(5):358-65.
18. Dégremont L, Azéma P, Maurouard E, Travers M-A. Enhancing resistance to *Vibrio aestuarianus* in *Crassostrea gigas* by selection. Aquaculture. 2020;526:735429.
19. Lasa A, di Cesare A, Tassistro G, Borello A, Gualdi S, Furones D, et al. Dynamics of the Pacific oyster pathobiota during mortality episodes in Europe assessed by 16S rRNA gene profiling and a new target enrichment next-generation sequencing strategy. Environ Microbiol. 2019;21(12):4548-62.
20. Mandas D, Salati F, Polinas M, Sanna MA, Zobba R, Burrai GP, et al. Histopathological and Molecular Study of Pacific Oyster Tissues Provides Insights into *V. aestuarianus* Infection Related to Oyster Mortality. Pathogens (Basel, Switzerland). 2020;9(6).
21. Garcia C, Mesnil A, Tourbiez D, Moussa M, Dubreuil C, Gonçalves de Sa A, et al. *Vibrio aestuarianus* subsp. *cardii* subsp. nov., pathogenic to the edible cockles *Cerastoderma edule* in France, and establishment of *Vibrio aestuarianus* subsp. *aestuarianus* subsp. nov. and *Vibrio aestuarianus* subsp. *francensis* subsp. nov. Int J Syst Evol Microbiol. 2021;71(2):004654.
22. Goudenège D, Travers MA, Lemire A, Petton B, Haffner P, Labreuche Y, et al. A single regulatory gene is sufficient to alter *Vibrio aestuarianus* pathogenicity in oysters. Environ Microbiol. 2015;17(11):4189-99.
23. Parizadeh L, Tourbiez D, Garcia C, Haffner P, Dégremont L, Le Roux F, et al. Ecologically realistic model of infection for exploring the host damage caused by *Vibrio aestuarianus*. Environmental Microbiology. 2018;20(12):4343-55.
24. Saulnier D, De Decker S, Haffner P. Real-time PCR assay for rapid detection and quantification of Vibrio aestuarianus in oyster and seawater: A useful tool for epidemiologic studies. Journal of Microbiological Methods. 2009;77(2):191-7.
25. Moran NA. Microbial minimalism: genome reduction in bacterial pathogens. Cell. 2002;108(5):583-6.
26. Floriano AM, Castelli M, Krenek S, Berendonk TU, Bazzocchi C, Petroni G, et al. The Genome Sequence of "Candidatus *Fokinia solitaria*": Insights on Reductive Evolution in Rickettsiales. Genome biology and evolution. 2018;10(4):1120-6.
27. Bäumler A, Fang FC. Host Specificity of Bacterial Pathogens. Cold Spring Harbor Perspectives in Medicine. 2013;3(12).
28. Siguier P, Gourbeyre E, Chandler M. Bacterial insertion sequences: their genomic impact and diversity. FEMS Microbiology Reviews. 2014;38(5):865-91.
29. Touchon M, Rocha EPC. Causes of Insertion Sequences Abundance in Prokaryotic Genomes. Molecular Biology and Evolution. 2007;24(4):969-81.
30. Labreuche Y, Le Roux F, Henry J, Zatylny C, Huvet A, Lambert C, et al. *Vibrio aestuarianus* zinc metalloprotease causes lethality in the Pacific oyster *Crassostrea gigas* and impairs the host cellular immune defenses. Fish & shellfish immunology. 2010;29(5):753-8.
31. Travers MA, Tourbiez D, Parizadeh L, Haffner P, Kozic-Djellouli A, Aboubaker M, et al. Several strains, one disease: experimental investigation of *Vibrio aestuarianus* infection parameters in the Pacific oyster, *Crassostrea gigas*. Vet Res. 2017;48(1):32.
32. Namouchi A, Didelot X, Schöck U, Gicquel B, Rocha EP. After the bottleneck: Genome-wide diversification of the Mycobacterium tuberculosis complex by mutation, recombination, and natural selection. Genome Res. 2012;22(4):721-34.

560 33. Claisse D, Alzieu C. Copper contamination as a result of antifouling paint
561 regulations? Marine Pollution Bulletin. 1993;26(7):395-7.
562 34. Hall LW, Anderson RD. A Deterministic Ecological Risk Assessment for Copper in
563 European Saltwater Environments. Marine Pollution Bulletin. 1999;38(3):207-18.
564 35. Rossi N, Jamet J-L. *In situ* heavy metals (copper, lead and cadmium) in different
565 plankton compartments and suspended particulate matter in two coupled Mediterranean
566 coastal ecosystems (Toulon Bay, France). Marine Pollution Bulletin. 2008;56(11):1862-70.
567 36. Weng N, Wang W-X. Variations of trace metals in two estuarine environments with
568 contrasting pollution histories. Science of The Total Environment. 2014;485-486:604-14.
569 37. Shi B, Wang T, Zeng Z, Zhou L, You W, Ke C. The role of copper and zinc
570 accumulation in defense against bacterial pathogen in the fujian oyster (*Crassostrea*
571 *angulata*). Fish & shellfish immunology. 2019;92:72-82.
572 38. Destoumieux-Garzón D, Canesi L, Oyanedel D, Travers M-A, Charrière GM, Pruzzo
573 C, et al. Vibrio–bivalve interactions in health and disease. Environmental Microbiology.
574 2020;22(10):4323-41.
575 39. Yeh S-T, Liu C-H, Chen J-C. Effect of copper sulfate on the immune response and
576 susceptibility to *Vibrio alginolyticus* in the white shrimp *Litopenaeus vannamei*. Fish &
577 shellfish immunology. 2004;17(5):437-46.
578 40. Bondarczuk K, Piotrowska-Seget Z. Molecular basis of active copper resistance
579 mechanisms in Gram-negative bacteria. Cell biology and toxicology. 2013;29(6):397-405.
580 41. Argüello JM, Raimunda D, Padilla-Benavides T. Mechanisms of copper homeostasis
581 in bacteria. Frontiers in cellular and infection microbiology. 2013;3:73.
582 42. Vanhove AS, Rubio TP, Nguyen AN, Lemire A, Roche D, Nicod J, et al. Copper
583 homeostasis at the host vibrio interface: lessons from intracellular vibrio transcriptomics.
584 Environ Microbiol. 2016;18(3):875-88.
585 43. Garcia C, Thébault A, Dégremont L, Arzul I, Miossec L, Robert M, et al. Ostreid
586 herpesvirus 1 detection and relationship with *Crassostrea gigas* spat mortality in France
587 between 1998 and 2006. Veterinary Research. 2011;42(1):73.
588 44. Barbosa Solomieu V, Renault T, Travers MA. Mass mortality in bivalves and the
589 intricate case of the Pacific oyster, *Crassostrea gigas*. J Invertebr Pathol. 2015;131:2-10.
590 45. Azéma P, Maurouard E, Lamy J-B, Dégremont L. The use of size and growing height
591 to improve *Crassostrea gigas* farming and breeding techniques against OsHV-1.
592 Aquaculture. 2017;471:121-9.
593 46. Azema P, Travers MA, De Lorgeril J, Tourbiez D, Degremont L. Can selection for
594 resistance to OsHV-1 infection modify susceptibility to *Vibrio aestuarianus* infection in
595 Crassostrea gigas? First insights from experimental challenges using primary and
596 successive exposures. Vet Res. 2015;46:139.
597 47. Azema P, Lamy JB, Boudry P, Renault T, Travers MA, Degremont L. Genetic
598 parameters of resistance to *Vibrio aestuarianus,* and OsHV-1 infections in the Pacific oyster,
599 *Crassostrea gigas*, at three different life stages. Genet Sel Evol. 2017;49(1):23.
600 48. Azéma P, Travers M-A, Benabdelmouna A, Dégremont L. Single or dual
601 experimental infections with *Vibrio aestuarianus* and OsHV-1 in diploid and triploid
602 *Crassostrea gigas* at the spat, juvenile and adult stages. Journal of Invertebrate Pathology.
603 2016;139:92-101.
604 49. Destoumieux-Garzón D, Matthies-Wiesler F, Bierne N, Binot A, Boissier J, Devouge
605 A, et al. Getting out of crises: Environmental, social-ecological and evolutionary research is
606 needed to avoid future risks of pandemics. Environment international. 2022;158:106915.

607 50. Anderson PK, Cunningham AA, Patel NG, Morales FJ, Epstein PR, Daszak P.
608 Emerging infectious diseases of plants: pathogen pollution, climate change and
609 agrotechnology drivers. Trends in Ecology & Evolution. 2004;19(10):535-44.
610 51. Buestel D, Ropert M, Prou J, Goulletquer P. History, status, and future of oyster
611 culture in France. Journal of Shellfish Research. 2009;28(4):813-20.
612 52. Håstein T, Hill BJ, Berthe F, Lightner DV. Traceability of aquatic animals. Revue
613 scientifique et technique (International Office of Epizootics). 2001;20(2):564-83.
614 53. Pernet F, Lupo C, Bacher C, Whittington RJ. Infectious diseases in oyster
615 aquaculture require a new integrated approach. Philosophical Transactions of the Royal
616 Society B: Biological Sciences. 2016;371(1689):20150213.
617 54. Wingett SW, Andrews S. FastQ Screen: A tool for multi-genome mapping and quality
618 control. F1000Research. 2018;7:1338.
619 55. Bush SJ. Read trimming has minimal effect on bacterial SNP-calling accuracy.
620 Microbial Genomics. 2020;6(12).
621 56. Bankevich A, Nurk S, Antipov D, Gurevich AA, Dvorkin M, Kulikov AS, et al. SPAdes:
622 a new genome assembly algorithm and its applications to single-cell sequencing. J Comput
623 Biol. 2012;19(5):455-77.
624 57. Gurevich A, Saveliev V, Vyahhi N, Tesler G. QUAST: quality assessment tool for
625 genome assemblies. Bioinformatics (Oxford, England). 2013;29(8):1072-5.
626 58. Kolmogorov M, Yuan J, Lin Y, Pevzner PA. Assembly of long, error-prone reads
627 using repeat graphs. Nature Biotechnology. 2019;37(5):540-6.
628 59. Vaser R, Sovic I, Nagarajan N, Sikic M. Fast and accurate de novo genome
629 assembly from long uncorrected reads. Genome Research. 2017.
630 60. Simão FA, Waterhouse RM, Ioannidis P, Kriventseva EV, Zdobnov EM. BUSCO:
631 assessing genome assembly and annotation completeness with single-copy orthologs.
632 Bioinformatics (Oxford, England). 2015;31(19):3210-2.
633 61. Seemann T. Prokka: rapid prokaryotic genome annotation. Bioinformatics (Oxford,
634 England). 2014;30(14):2068-9.
635 62. Cantalapiedra CP, Hernández-Plaza A, Letunic I, Bork P, Huerta-Cepas J. eggNOG-
636 mapper v2: Functional Annotation, Orthology Assignments, and Domain Prediction at the
637 Metagenomic Scale. Molecular Biology and Evolution. 2021;38(12):5825-9.
638 63. Huerta-Cepas J, Szklarczyk D, Heller D, Hernández-Plaza A, Forslund SK, Cook H,
639 et al. eggNOG 5.0: a hierarchical, functionally and phylogenetically annotated orthology
640 resource based on 5090 organisms and 2502 viruses. Nucleic Acids Research.
641 2018;47(D1):D309-D14.
642 64. Xie Z, Tang H. ISEScan: automated identification of insertion sequence elements in
643 prokaryotic genomes. Bioinformatics (Oxford, England). 2017;33(21):3340-7.
644 65. Syberg-Olsen MJ, Garber AI, Keeling PJ, McCutcheon JP, Husnik F. Pseudofinder:
645 detection of pseudogenes in prokaryotic genomes. bioRxiv. 2021:2021.10.07.463580.
646 66. Goris J, Konstantinidis KT, Klappenbach JA, Coenye T, Vandamme P, Tiedje JM.
647 DNA-DNA hybridization values and their relationship to whole-genome sequence similarities.
648 Int J Syst Evol Microbiol. 2007;57(Pt 1):81-91.
649 67. Darling AE, Mau B, Perna NT. progressiveMauve: Multiple Genome Alignment with
650 Gene Gain, Loss and Rearrangement. PLOS ONE. 2010;5(6):e11147.
651 68. Page AJ, Taylor B, Delaney AJ, Soares J, Seemann T, Keane JA, et al. SNP-sites:
652 rapid efficient extraction of SNPs from multi-FASTA alignments. Microbial Genomics.
653 2016;2(4).

654 69. Didelot X, Wilson DJ. ClonalFrameML: Efficient Inference of Recombination in Whole
655 Bacterial Genomes. PLOS Computational Biology. 2015;11(2):e1004041.
656 70. Tajima F. Statistical method for testing the neutral mutation hypothesis by DNA
657 polymorphism. Genetics. 1989;123(3):585-95.
658 71. Paradis E. pegas: an R package for population genetics with an integrated–modular
659 approach. Bioinformatics (Oxford, England). 2010;26(3):419-20.
660 72. Petton B, Pernet F, Robert R, Boudry P. Temperature influence on pathogen
661 transmission and subsequent mortalities in juvenile Pacific oysters *Crassostrea gigas*.
662 Aquaculture Environment Interactions. 2013;3(3):257-73.
663

664

665 Table 1: **Analysis of molecular variance** supported genetic partitioning according to

666 environmental origin and isolation context

Factor	*Variability (%)*	*p-value*
Environmental origin	**17.8**	**0.002**
Isolation context	**16.0**	**0.001**
Country of isolation	7.1	0.074
Year of isolation	3.4	0.25

667

668

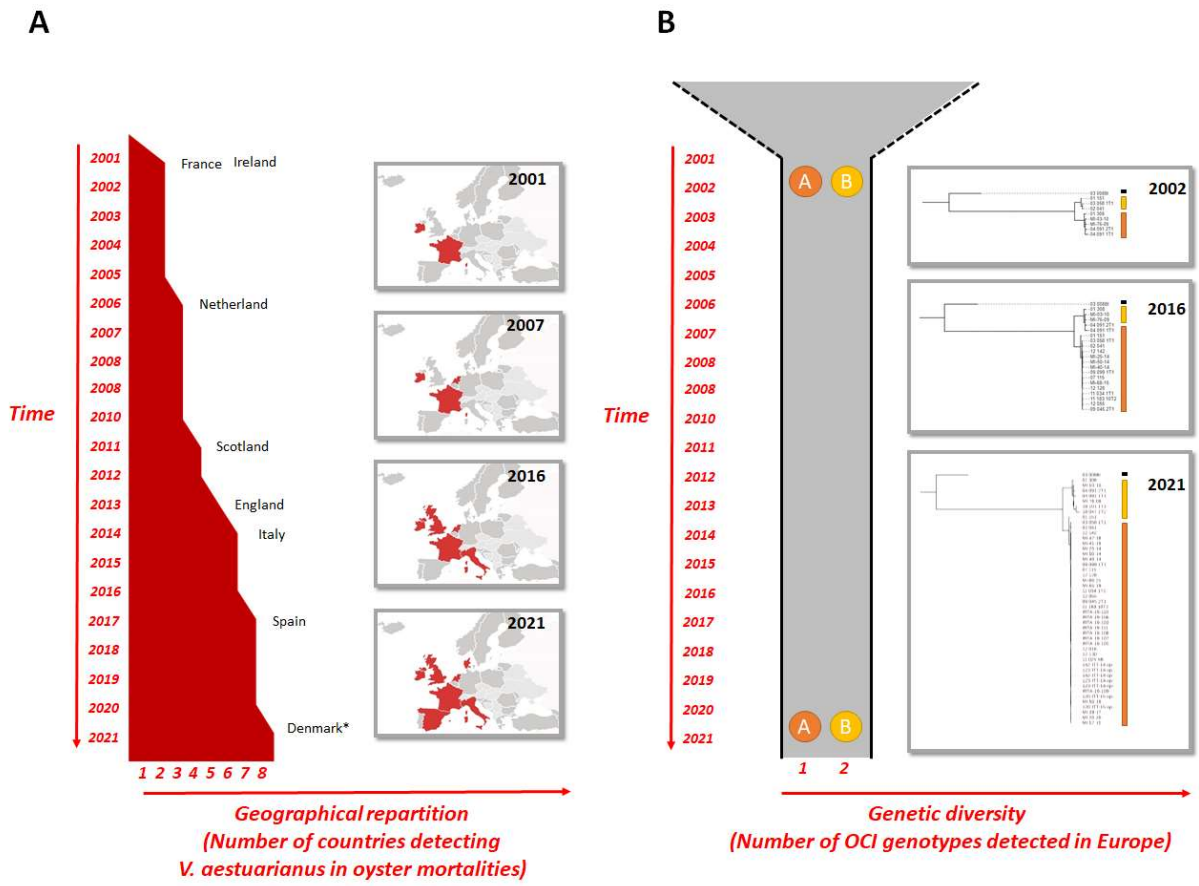

669

670 Figure 1: **European expansion of *V. aestuarianus francensis***. While the geographic

671 distribution of *V. aestuarianus* strains involved in *C. gigas* mortalities expands, genetic

672 diversity remains stable over time. A: The number of countries reporting the detection of *V.*

673 *aestuarianus* was assessed through a questionnaire sent to European national reference

674 laboratories (NRLs). *Note that the Denmark case report corresponds to a suspected case

675 without bacterial isolation. B: The two lineage expansions: 2 genotypes were determined

based on a maximum likelihood phylogenetic tree from complete genome alignments (GTR substitution model).

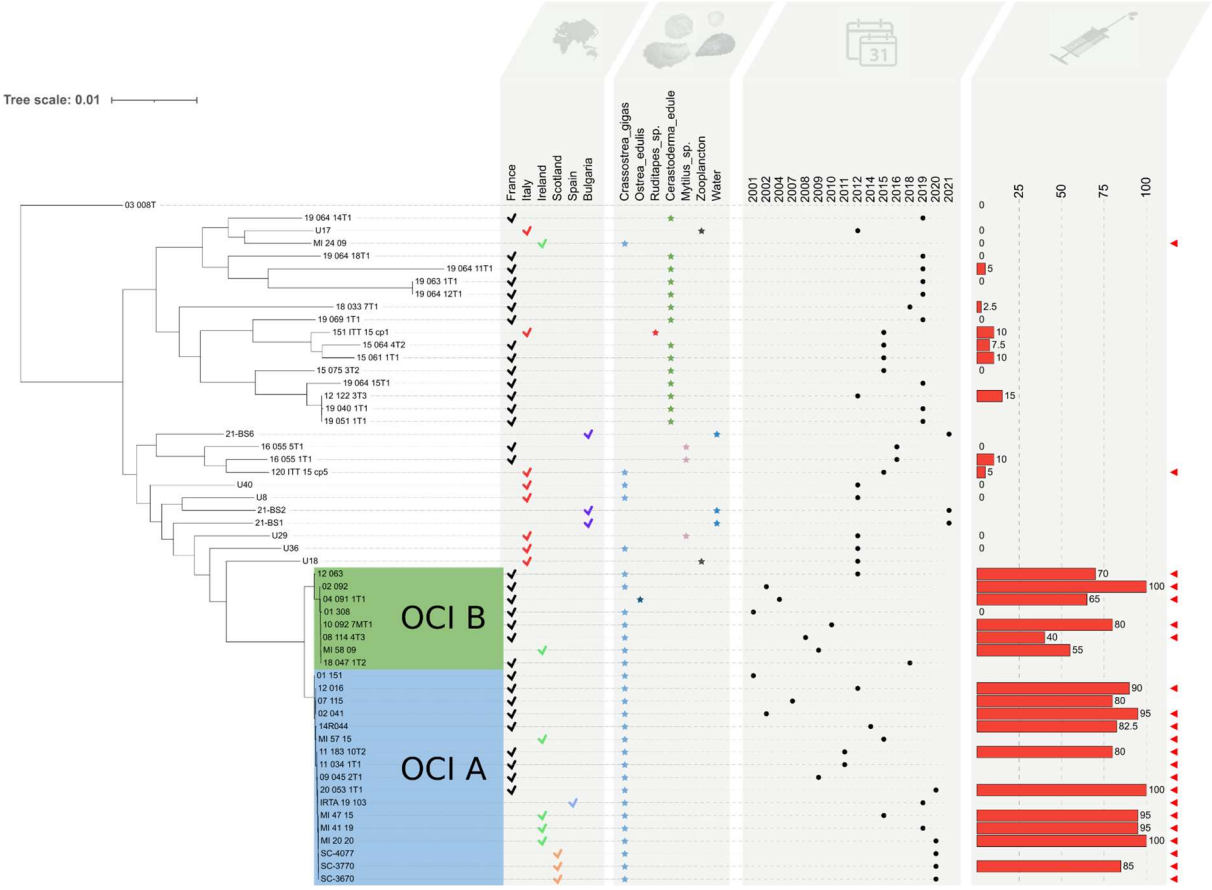

Figure 2: ***V. aestuarianus* diversity is structured according to host species and isolation context.** Phylogenetic tree of *V. aestuarianus* species calculated with RAxML using a GTR substitution model and rooted with the 03_008T strain (outgroup) from whole-genome alignments. Several layers of annotations are added: country (check mark), matrix of isolation (star), year of isolation (point), virulence testing in the laboratory by injection into oysters (10^7 UFC/animal) indicated with a bar plot on the right side representing mortality percentages, and context (strains isolated during oyster mortality events are indicated with a red arrow on the right). Oyster clinical isolate (OCI) clades A and B are highlighted in blue and green, respectively. The absence of virulence data means the absence of a test for this strain.

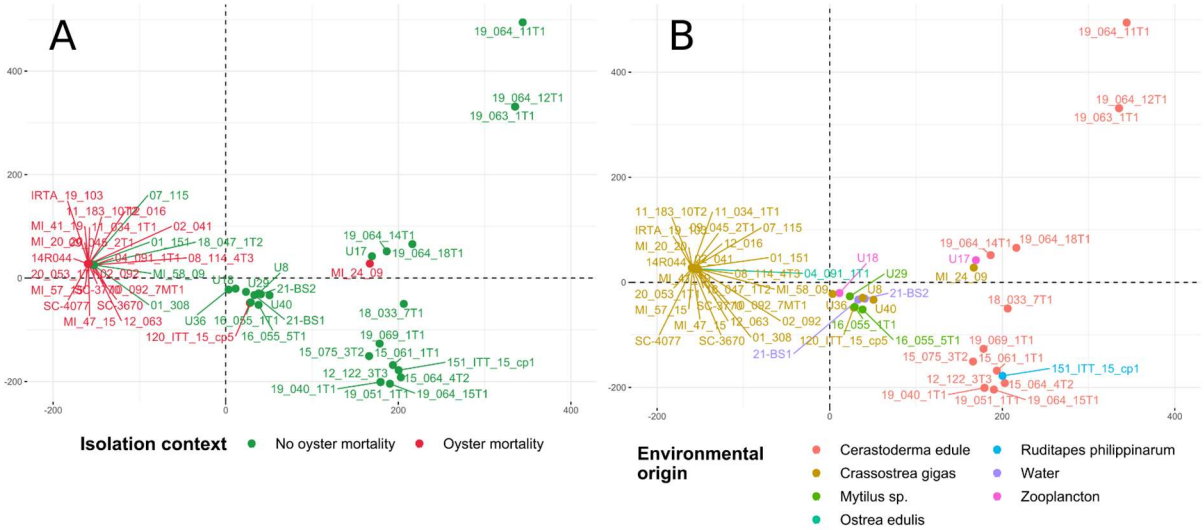

Figure 3: **Principal component analysis (PCA) of genetic polymorphism segregates *V. aestuarianus* isolates according to environmental origin and isolation context**, according to genome-wide analysis of 54 genomes using 183 109 SNPs. PC1 and PC2 represent the first two eigenvectors from the PCA. Isolates are colored according to the isolation context (A) and according to the environmental origin (B). PC1 and PC2 explain 16.7% and 9.2% of the variability between samples, respectively.

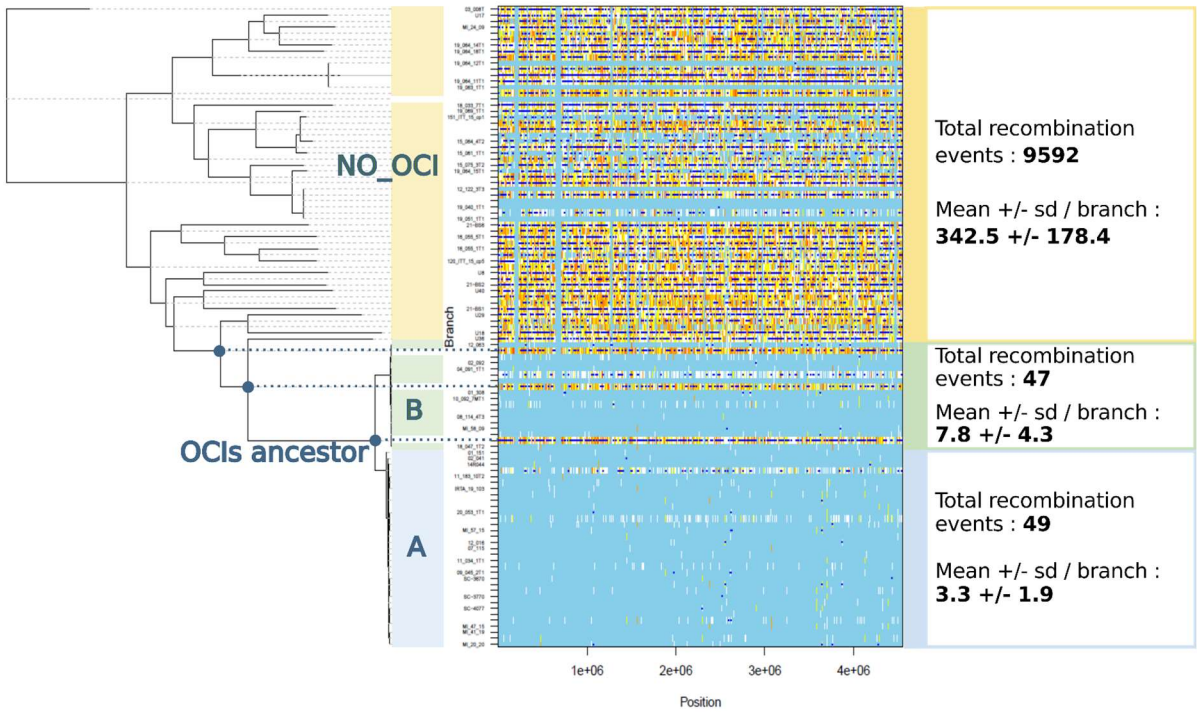

Figure 4: **A limited number of recombination events occurred in oyster clinical isolate**

698 **(OCI) genomes after their expansion.** Detected **recombination** events are shown by dark
699 blue horizontal bars. For a given branch, light blue sites indicate no substitution. All other
700 colors (from white to red) indicate a substitution. White represents a nonhomoplasic
701 substitution. An increasing level of redness means an increasing degree of homoplasy. OCI
702 clades A and B are represented in blue and green, respectively, and the NO_OCI group is
703 shown in yellow. For improved readability, some nodes of the tree as well as the row of the
704 recombination events matrix related to these nodes are indicated with points and dashed
705 lines. The strain 03_008T sequence was used as a reference.

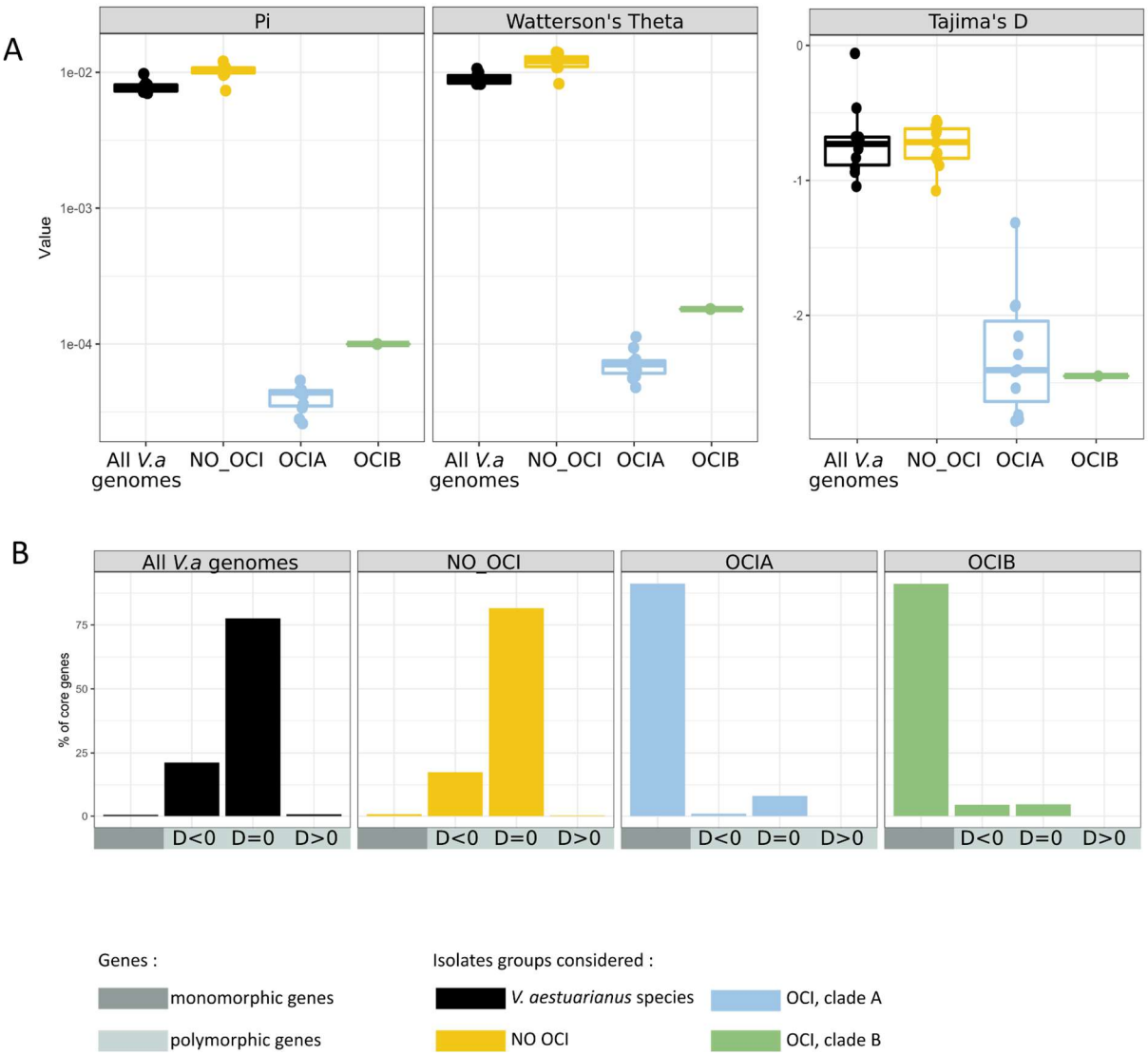

706

707 Figure 5: **Strong impact of purifying selection on oyster pathogens.** Genetic statistics in
708 *V. aestuarianus* species (black), NO_OCI (yellow), oyster clinical isolates (OCIs), clade A

709 (blue) and clade B (green). **A: Whole genome scale**. Even through the expected genetic
710 diversity under neutral evolution and a stable population size in OCIs is low (Watterson's
711 theta), the observed diversity (Pi) is still lower, as shown by the Tajima's D value below -2.
712 For *V. aestuarianus*, OCI_A and NO_OCI, 10 random subsamples of 8 sequences in each
713 alignment were examined to avoid bias due to differences in the number of sequences. For
714 the OCI_B alignment, the 8 sequences represent the entire sampled set. Pi: observed
715 genetic diversity; Theta_w: Watterson estimate of expected genetic diversity; Tajima_D:
716 Tajima's D test statistic. The Y axis in the Pi and Watterson's theta plots is log10 scaled.
717 **B: Gene scale**. Core genes show different selection patterns among groups of strains and
718 among core genes within groups. While most core genes are under neutral evolution in
719 isolates other than OCIs, most genes are monomorphic in OCI clades A and B. D>0 and
720 D<0: significantly negative or positive Tajima's D value ($p < 0.05$) and D=0 ($p > 0.05$). A
721 negative Tajima's D is indicative of purifying selection or recent population expansion, while
722 a positive Tajima's D is indicative of diversifying selection or population contraction. A zero
723 value is indicative of neutral evolution.
724

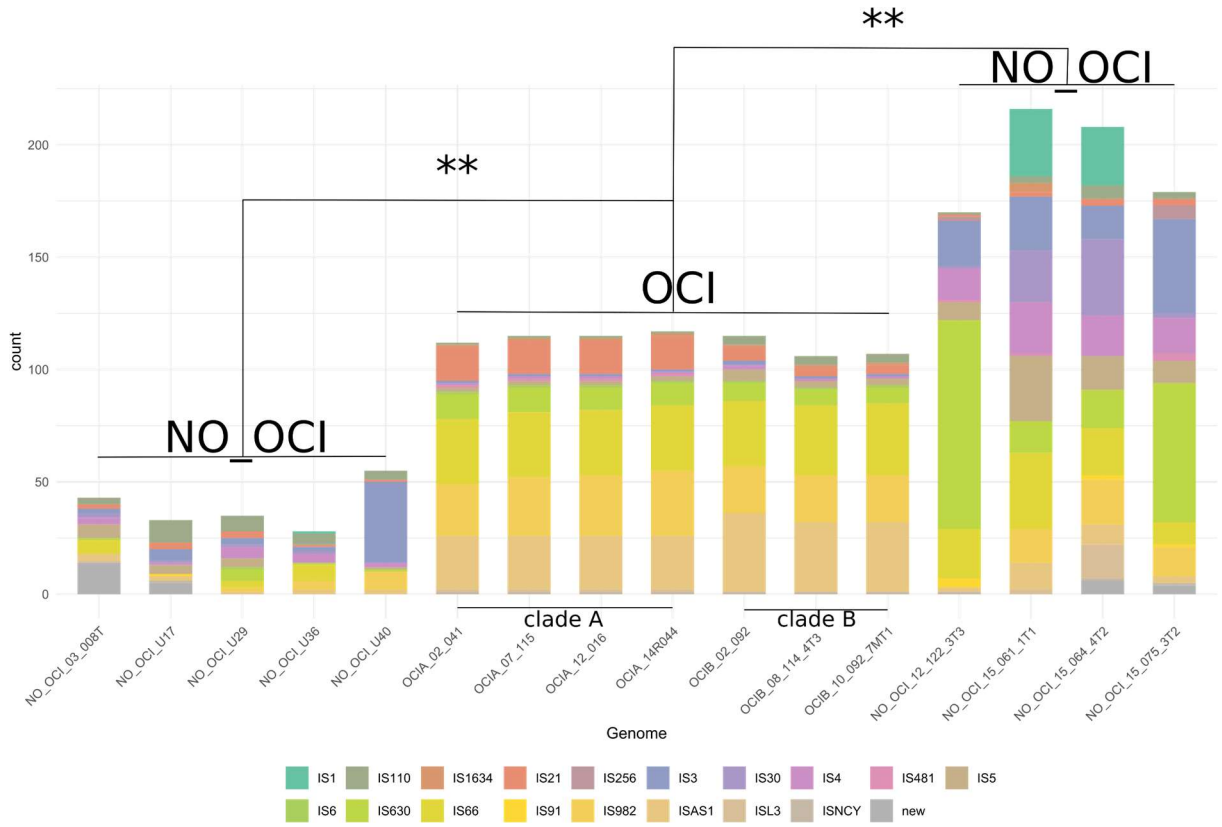

Figure 6: **Differential Insertion sequence (IS) enrichment is observed in oyster clinical isolate (OCI) genomes and cockle associated NO-OCI.** Distribution of the number of IS elements (complete and partial) in 16 complete genomes (chromosomes A and B). Colors represent IS families predicted by ISEScan. The genomes are those of 4 OCI clade A strains, 3 OCI clade B strains, 5 NO_OCI strains isolated independent of bivalve mortality (NO_OCI group 1), and 4 NO_OCI strains isolated during cockle mortality events (NO_OCI group 2). The conservation of IS number and families between genomes of OCIs from clade A or clade B indicates an ancestral origin of ISs. The genomes that contain the most ISs are those of strains isolated during cockle mortality events (NO_OCI group 2). The diversity of IS quantities and families represented suggests that IS enrichment is in progress. The number of ISs in groups was significantly different between OCI and NO_OCI from group 1 and group 2 (**: Kruskal test p value < 0.05).

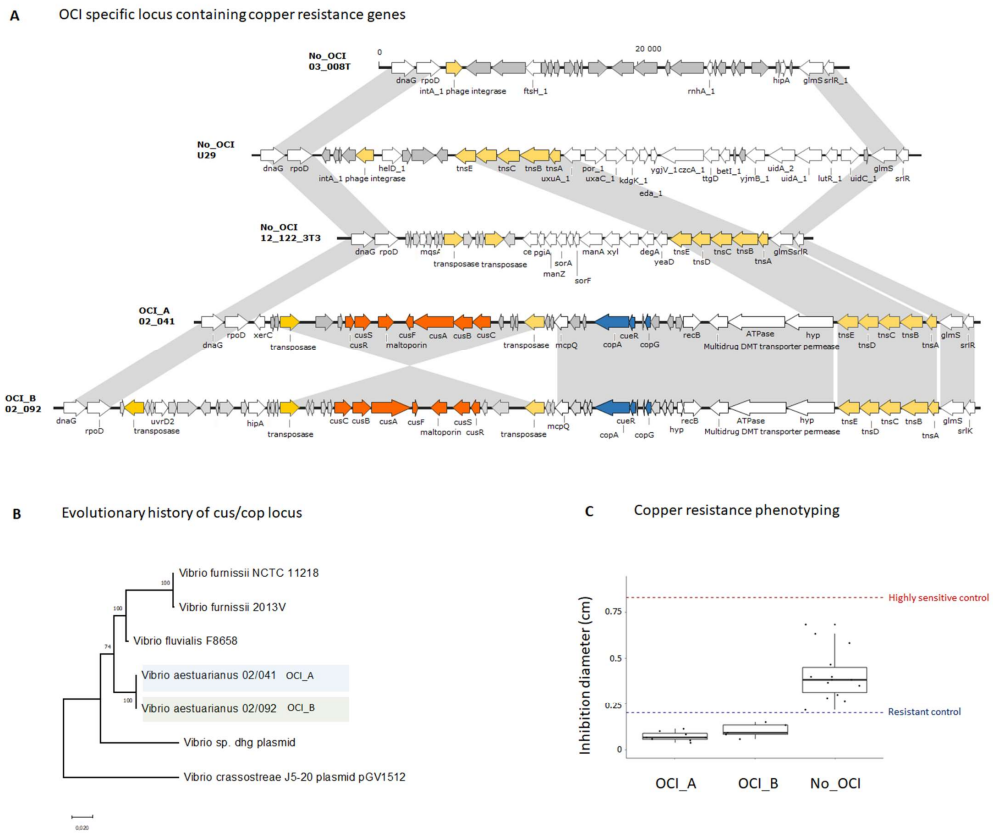

739

740 Figure 7: A. Oyster clinical isolate (OCI)-specific locus containing copper resistance genes.
741 Transposase and integrase are indicated in yellow, cus genes in orange, and cop genes in
742 blue.
743 B. Evolutionary history of the cus/cop locus. NJ, bootstrap test (500 replicates). The
744 evolutionary distances were computed using the Kimura 2-parameter method [3] and are
745 shown as the number of base substitutions per site. This analysis involved 8 nucleotide
746 sequences. All ambiguous positions were removed for each sequence pair (pairwise deletion
747 option). There were a total of 29 555 positions in the final dataset. Evolutionary analyses
748 were conducted in MEGA X [4]. C. Agar plate assay: bacterial growth inhibition diameter
749 around a pellet impregnated with 50 mM $CuSO_4$ solution.
750